Supporting Information

An RNA aptamer-based microcantilever sensor to detect the inflammatory marker, mouse lipocalin-2

Lijie Zhai[†,§a] Tianjiao Wang[†,a,] Kyungho Kang[‡], Yue Zhao[‡], Pranav Shrotriya[‡], Marit Nilsen-Hamilton[†,*]

[†]Department of Biochemistry, Biophysics and Molecular Biology and [‡]Department of Mechanical Engineering, Iowa State University, Ames, Iowa 50011, USA. [§]current address: Dept of Pediatrics, University of Chicago, Chicago, IL 60637

* CORRESPONDING AUTHOR: Marit Nilsen-Hamilton, 3206 Molecular Biology Building, Dept of Biochemistry, Biophysics and Molecular Biology, Iowa State University, Ames, IA 50011; Phone: 515-294-9996; Fax: 515-294-0453; Email: marit@iastate.edu

[a] co-first authors with equal contributions

MATERIALS AND METHODS

Preparation of mLcn2-Resin

His-tagged proteins were captured on Talon cobalt affinity resin (Clontech) in the buffer containing 50 mM KH_2PO_4, 150 mM NaCl, 0.02% NaN_3, 0.05% Tween-20, pH 7.4. The unbound proteins were removed by washing the resin with the buffer 3 times. The protein-resin coupling efficiency was calculated by determining the protein concentrations in the original protein prep and the flow-through and washes. Protein-resin was stored as a 50% slurry in the above buffer at 4 ºC with a concentration at 0.70 mg mLcn2 per ml beads. A 50% slurry of the resin without addition of the proteins was prepared according to the same procedure and used as the negative control for the *in vitro* aptamer selection.

In Vitro Selection of Aptamers

In vitro selection of an aptamer for mLcn2 was carried out by SELEX (Systematic Evolution of Ligands by EXponential enrichment).[1] A ds-DNA library was generated from the ss-DNA

library (oligo 487) by Taq polymerase extension using oligo 484 as a primer. The reaction was carried out at 72 ºC in 2 ml mixture of 1.67 μM oligo487, 3.33 μM oligo484, 0.5 mM dNTP, 50 mM KCl, 10 mM Tris (pH 9.0 at 25 ºC), 1.5 mM $MgCl_2$, 0.1% Triton X-100 and 0.05 U/μl Taq polymerase . The starting dsDNA pool was resolved by 8% polyacrylamide gel electrophoresis and purified by passive diffusion from the gel. The dsDNAs from later rounds of selection were purified with QIAquick PCR purification kit (Qiagen). The purified dsDNAs (360 pmol for the first round and 1/3 of the PCR products for the rest rounds) were *in vitro* transcribed in 40-80 μl mixture of 30 mM Tris, 10 mM DTT, 2 mM spermidine, 20 mM Triton X-100, 20 mM $MgCl_2$, pH 8.5, 5 mM each of ATP, GTP, UTP, CTP, 0.7 μM T7 RNA polymerase, 0.2 U/ml inorganic pyrophosphatase (New England Biolabs) at 42 ºC for 1 hour. For the 1st, 6th, 9th and 10th rounds of selection, 10 μCi α-^{32}P-ATP (6000 Ci/mmol) was added to the reaction mixture to prepare radioisotope labeled transcripts for monitoring RNA binding to mLcn2 on talon-resin. The reactions were stopped by the addition of 20-40 U of RNase free DNase I followed by incubation at 37 ºC for 30 min. The transcribed RNA was precipitated by ethanol and subsequently dissolved in 20-50 μl of 7M urea prior to being fractionated by denaturing (7 M urea) polyacrylamide gel electrophoresis (PAGE; 8% acrylamide:bisacrylamide, 19:1, w/v) in buffer containing 45 mM Tris/borate (pH 7.5) and 1 mM EDTA. RNA products were then visualized by UV-shadowing, and the bands corresponding to the full-length RNAs were excised. The transcripts were eluted by a solution of 0.3 M sodium acetate and 1 mM EDTA from the gel slices overnight at 23 ºC. The elution was extracted twice with phenol/chloroform followed by ethanol precipitation. The final RNA was dissolved in 20-30 μl deionized water and the RNA concentration was determined by NanoDrop at 260 nm.

The transcribed RNAs were diluted in a selection buffer of 50 mM KH_2PO_4, 150 mM NaCl, 5 mM $MgCl_2$, pH 7.4 and loaded onto a column containing 0.2 ml of mLcn2-resin equilibrated with the same buffer. For the 3rd, 6th and 9th rounds of selection, the RNAs were first loaded onto

column containing only resin without mLcn2 as a negative selection. The columns were rinsed with 300 µl of selection buffer and the eluates (unbound RNAs) were then loaded on to a second column containing 0.2 ml mLcn2-resin. For the positive selection, the protein and RNA concentration started at 7.8 µM and 16 µM respectively in a 200 µl reaction volume and was incrementally decreased to reach 0.90 µM and 1.2 µM respectively in a 500 µl volume at round 10. Following 1 h of incubation at room temperature, the columns were washed with 5 to 10 ml of selection buffer and the mLcn2-RNAs complex was eluted with 150 mM imidazole (pH 7.4). Eluted RNAs were extracted twice with phenol/chloroform followed by ethanol precipitation.

Aliquots of the above purified RNAs (1/3 volume) were reverse transcribed by ThermoScript reverse transcriptase using oligo 485 as the primer. The reverse transcription (RT) was carried out in 20 µl mixture of dNTPs (1mM each), 2.5 µM oligo 485, 0.75 U/µl reverse transcriptase, 50 mM Tris acetate (pH 8.4 at 25 ºC), 75 mM potassium acetate, 8 mM magnesium acetate. Half of the reverse-transcribed cDNAs were amplified by PCR in 100 µl mixture of 50 mM KCl, 10 mM Tris (pH 9.0 at 25 ^{0}C), 1.5 mM $MgCl_2$, 0.1% Triton X-100 and 0.025 U/µl Taq polymerase, dNTPs (0.2 mM each), 2 µM reverse primer oligo 484 and 2 µM forward primer oligo 485 with the temperature control of 1 cycle of 93 ºC, 3 min; 6-12 cycles of 93 ºC, 30 sec, 65 ºC, 1 min, 72 ºC, 1min and 1 cycle of 72 ºC, 7 min. These described rounds of *in vitro* transcription, RNA-protein binding and partition and RT-PCR were carried out until significant enrichment of RNA binders was observed. At round 10, the enriched pool was cloned into pCR-XL-TOPO vector for sequencing and further characterization.

Binding Affinity Measurement

Filter binding assay

A standard filter binding assay was used to determine the K_ds of the aptamers for $Fe(DHBA)_3$ or mLcn2 interactions and to study the competition between the aptamer and $Fe(DHBA)_3$ for mLcn2 binding at 23 ^{0}C. The $^{55}Fe(DHBA)_3$ was prepared by mixing 0.5 mM

$^{55}FeCl_3$, 1.5 mM DHBA, 0.1 mM Tris (pH 8.0 at 25 ^{0}C) for 30' at 23 ^{0}C. For the competition assay and K_d measurement of the $Fe(DHBA)_3$ – mLcn2 interaction, the buffer was 50 mM Tris, 150 mM NaCl, 10 mM $CaCl_2$, 5 mM $MgCl_2$, pH 7.4. For the K_d measurement of aptamer – mLcn2 interaction, the buffer was 50 mM KH_2PO_4, 150 mM NaCl, 5 mM $MgCl_2$, pH 7.4. Briefly, 50 µl samples for binding or competition assays were filtered through a 96-well filtration apparatus (Bio-Rad) assembled with buffer soaked nitrocellullose membrane (GE Water & Process Technologies) on top of buffer soaked, positively charged nylon membrane (Millipore) by 55 cm Hg vacuum. The membranes were then washed three times with 0.5 ml of buffer and air-dried. The radioisotope on the membranes was recorded on a phosphor screen, scanned by Typhooon 8600 Variable Model Imager (GE Health Care Life Sciences) and quantified by ImageQuant (GE Health Care Life Sciences). The percent bound was calculated as the ratio of the intensity on the nitrocellulose membrane to that of the sum on nitrocellulose membrane and nylon membrane. For every filter binding assay, each sample was performed in duplicate or triplicate.

Isothermal titration calorimetry (ITC)

ITC experiments were performed using a Nano-ITC isothermal titration calorimeter (TA Instrument). In each experiment, 50 µM of aptamer dissolved in the binding buffer was titrated using the computer-controlled syringe into the sample cell (0.95 mL) containing either binding buffer or 5 µM mLcn2 dissolved in the same buffer at 25 ºC. The syringe was set at a stirring speed of 150 rpm. After a 60 s initial delay, each titration involved an initial 1 µL injection followed by 15 serial injections of 15 µL at intervals of 300 s. The raw data obtained in each experiment were corrected for the effect of titrating aptamer from the syringe to the sample cell containing the buffer only but no protein. The thermodynamic parameters were calculated using a one-site binding model in the analysis software (NanoAnalyze) provided by TA Instruments.

Circular Dichroism (CD)

CD measurements were performed with a Jasco J-710 spectropolarimeter. The samples were scanned in the far-UV wavelength range from 190–250 nm in a quartz cell with a path-length of 0.1 cm at 22 ºC. All experiments were performed in 10 mM Na_2HPO_4, pH 7.4. CD values after buffer background subtraction were used as the final reading for each protein sample. The raw CD readings were input into CDFit (http://www.ruppweb.org/cd/cdtutorial.htm#Program%20CDFIT) to calculate the mean molar ellipticity per residue and to predict the secondary structure.

Size Exclusion Chromatography and non-reducing polyacrylamide gel electrophoresis

Protein samples in either filter binding buffer (50 mM KH_2PO_4, 150 mM NaCl, 5 mM $MgCl_2$, pH 7.4) or CD buffer (10 mM Na_2HPO_4, pH 7.4) were loaded onto a Superdex G75 column and the chromatography were performed at 4 ºC with a flow rate at 0.4ml/min. For determination of stoichiometry, the oligonucleotides and the protein samples were dissolved in the filter binding buffer. The non-reducing native PAGE was performed same way as regular SDS-PAGE but in the absence of SDS and reducing agents. In addition, samples were not heated prior to the non-reducing native PAGE in contrast to samples for SDS-PAGE.

Computational simulations

The 3-D structure of mLcn2 was predicted based on homologous modeling using SWISS-MODEL following program instructions. The surface amino acids were identified as amino acids that are more than 30% solvent accessible as analyzed by the Swiss Pdb-Viewer. The secondary structures of RNA aptamers were predicted by both Sfold (Srna module) (**http://sfold.wadsworth.org**) and MC-FOLD (http://www.major.iric.ca/MC-Pipeline/) using the aforementioned experimental conditions as prediction parameters.[2] After this work was completed the crystal structure of mLcn2 was deposited in the database and found to match the homology-based simulation.[3]

Supplemental Table 1

Oligo Number	Use	Oligo Sequence (5' to 3')
Oligo 487	Random ssDNA pool	GCCTGTTGTGAGCCTCCTGTCGAA(N53)TTGAGCGTTTATTCTTGTCTCCC
Oligo 484	reverse primer for SELEX	TAATACGACTCACTATAGGGAGACAAGAATAAACGCTCAA
Oligo 485	forward primer for SELEX	GCCTGTTGTGAGCCTCCTGTCGAA
Oligo 258	negative control for $Fe(DHBA)_3$ competition binding	GGAUCCCGACUGGCGAGAGCCAGGUAACGAAUGGAUCC
Cantilever reference oligo	negative control oligo for reference cantilever	GTGAGAGAAGACGCGTAA
Oligo 569	original mLcn2 aptamer	CCUCCGGCUCAUACCUUUUCGAAGACAAGCUUCGACAGGAGG
Oligo 571[a]	mutated mLcn2 aptamer	CCGCCGGCUCAUACCUUUUCGAAGACAAGCUUCGACAGGCGG
Oligo 572		CCUCCGGCUCAUGCCUUUUCGAAGACAAGCUUCGACAGGAGG
Oligo 573[b]		CCUCCG–CUCAUA—UUUUCGAAGACAAGCUUCGACAGGAGG
Oligo 576[c]		**GG**CCGCCGGCUCAUACCUUUUCGAAGACAAGCUUCGACAGGCGG**CC**
Oligo 577		CCUCCGGCUCAUACCUUUUCGAAGCUAACCUUCGACAGGAGG
Oligo 578		CCUCCGGCUCAUACCUUUUGUCAGACAAGCUGACACAGGAGG
Oligo 579		CCUCCGGCUCAUACCAAUUCGAAGACAAGCUUCGACAGGAGG
Oligo 580		CCUCCGGCUCAUACCUUUUCGAAGACAAGCUUCGAUAGGAGG

a: Underlined residues are substitution for original nucleosides
b: Hyphen represents residue deletion
c: Residues in bold represent addition to original sequence

Supplemental Table 2

protein	**10mM NaH_2PO_4, pH6.5**	**50mM Tris, 0.15M NaCl, 5mM MgCl, pH7.2**
mLcn2	11.6	13.0
R103A	10.0	12.9
R103A_K147A	10.1	12.8
R103A_K147A_K156A	10.5	12.8
H120A	ND	12.8

LEGEND: The size exclusion chromatography analysis of the WT mLcn2 and some mLcn2 mutants was performed in two buffers. Shown are the post-V_o elution volumes. The elution volume shift of mutants compared with WT was observed in both buffers. ND, not determined.

LEGENDS TO FIGURES

Figure S1. Binding to mLcn2 of some putative aptamers and their truncated derivatives. The full length of A1 and A4 and their truncated derivatives (oligo 569 from A1, oligo 570 from A4) based on the 3-way junction structures were tested for the binding to mLcn2 using the filter binding assay.

Figure S2. Raw data for isothermal titration calorimetry analysis of binding of oligo569 to mLcn2. ITC was performed as described in Figure 2C. Raw data from the aptamer titration to buffer (**left panel**) and aptamer titration to mLcn2 (**right panel**) were shown Each peak represents one injection. The figure shows one representative result from two independently performed experiments.

Figure S3. Analysis of mLcn2-oligo569 stoichiometry by gel filtration. The binding stoichiometry of the mLcn2 to oligo 569 was also investigated using size-exclusion chromatography. The oligo 569 alone or in combination with mLcn2 in a molar ratio of 2:1 were subjected to the chromatography using Superdex G75 column with mLcn2 alone as another control. The elution buffer was 50 mM Tris, 150 mM NaCl, 5 mM $MgCl_2$, pH7.2. The molecular masses shown above the peaks were calculated using the same regression line as in Figure S6. They are: mLcn2 (18 kDa), oligo569 (19 kDa) and the new peak containing the mLcn2-oligo569 complex (33 kDa).

Figure S4. Predicted secondary structure of oligo 569. The consensus secondary structures of oligo 569 predicted by S-fold and MC-folds are shown.

Figure S5. Similar three-way junction structures predicted of all aptamer variants by S-fold and MC-Fold. An ensemble of secondary structures of 8 putative mLcn2 aptamer variants (oligo 571 to oligo 580) as predicted by MC-Fold and S-Fold.

Figure S6. Circular dichroism spectra of mLcn2 and mutants. A) wild-type mLcn2 and mutant mLcn2 containing alanine replacement mutants of R103, K147 and K156. Shown are the average mean molar elipticity per residue from 4-7 independently gathered scans. **B)** The

percentage of secondary structures for each mutant obtained by fitting the average CD data from A. These results show that alanine replacement of these calyx-exposed amino acids have no measurable effect on the global conformation of mLcn2.

Figure S7. Analysis of mLcn2 mutants by gel electrophoresis and gel filtration to assess their structural integrity. The recombinant mLcn2 and selected mutants of its surface amino acids and siderophore binding sites were analyzed by size exclusion chromatography through a Superdex G75 column and non-reducing native polyacrylamide gel electrophoresis. The eluted peaks of the core mutants and the wild-type mLcn2 are shown in an overlapping view with their calculated molecular mass. The regression line was generated using protein standards: bovine serum albumin (64.0KDa), carbonic anhydrase (30.0KDa), myoglobin (17.7KDa) and cytochrome C (12.5KDa). The elution buffer was 10 mM NaH_2PO_4, pH 6.

S8: Comparison of $Fe(DHBA)_3$ binding by various proteins to establish the level of nonspecific binding. Recombinant mLcn2, hLcn2, Ex-FABP, bovine serum albumin were incubated with $Fe(DHBA)_3$ at a ratio of 2:1 $Fe(DHBA)_3$ to protein with the protein concentration being: 40 μM hLcn2 and mLcn2, 90 μM Ex-FABP and 30 μM BSA. The optical density was measured at 540 nm to determine $Fe(DHBA)_3$ binding. The buffer was 20 mM NaCl, 10 mM phosphate, pH7.7.

Figure S9. Sequence alignment of human and mouse lipocalin-2. The 3 iron-siderophore binding residues (red rectangles) are located in conserved regions of Lcn2 (yellow: identical amino acids; green: similar amino acids). The residues in the siderophore binding pocket (blue rectangles) are also conserved between hLcn2 and mLcn2.

CITATIONS

1. T. Fitzwater, B. Polisky, *Methods Enzymol* 1996, *267*. 275-301
2. (a) Y. Ding, C. Y. Chan, C. E. Lawrence, *RNA* 2005, *11*. 1157-66; (b) Y. Ding, C. E. Lawrence, *Nucleic Acids Res* 2003, *31*. 7280-301; (c) M. Parisien, F. Major, *Nature* 2008, *452*. 51-5
3. A. D. Bandaranayake, C. Correnti, B. Y. Ryu, M. Brault, R. K. Strong, D. J. Rawlings, *Nucleic Acids Research* 2011, *39*. e143

Figure S1

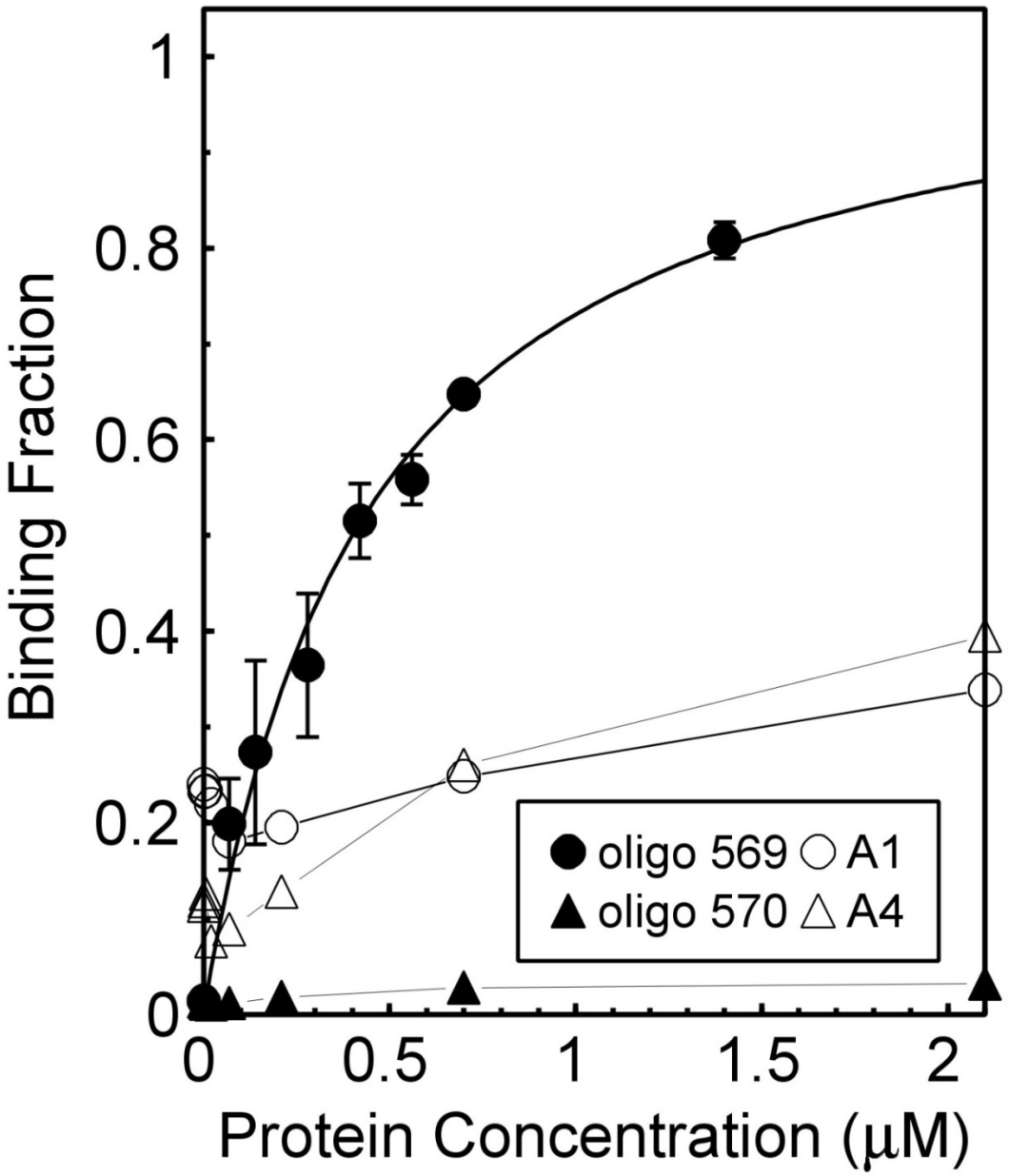
Binding Fraction
Protein Concentration (μM)
0
0.2
0.4
0.6
0.8
1
0
0.5
1
1.5
2
oligo 569
A1
oligo 570
A4

Figure S2

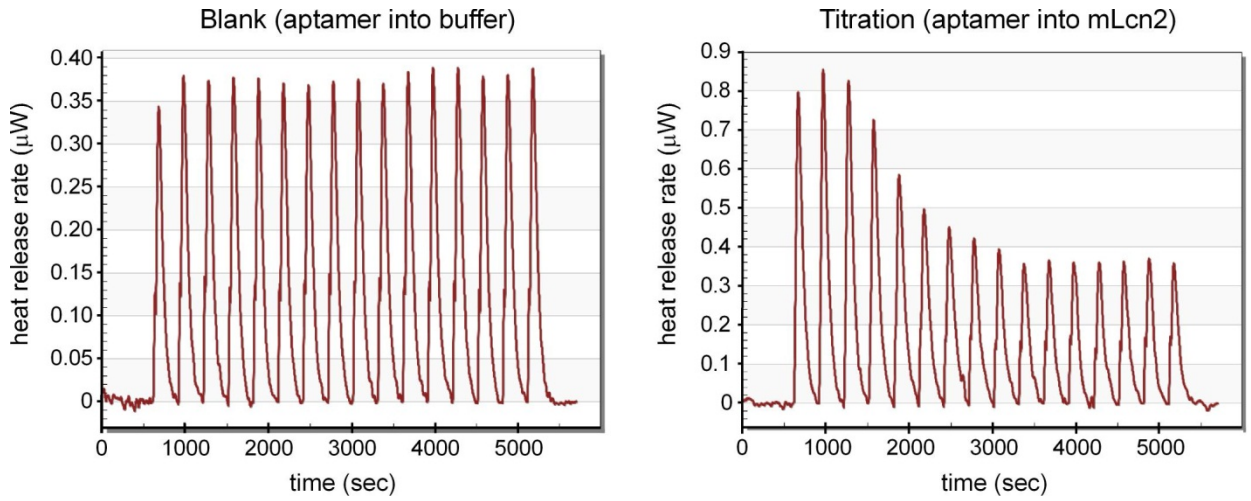
Blank (aptamer into buffer)
heat release rate (μW)
0.40
0.35
0.30
0.25
0.20
0.15
0.10
0.05
0
0
1000
2000
3000
4000
5000
time (sec)
Titration (aptamer into mLcn2)
heat release rate (μW)
0.9
0.8
0.7
0.6
0.5
0.4
0.3
0.2
0.1
0
0
1000
2000
3000
4000
5000
time (sec)

Figure S3

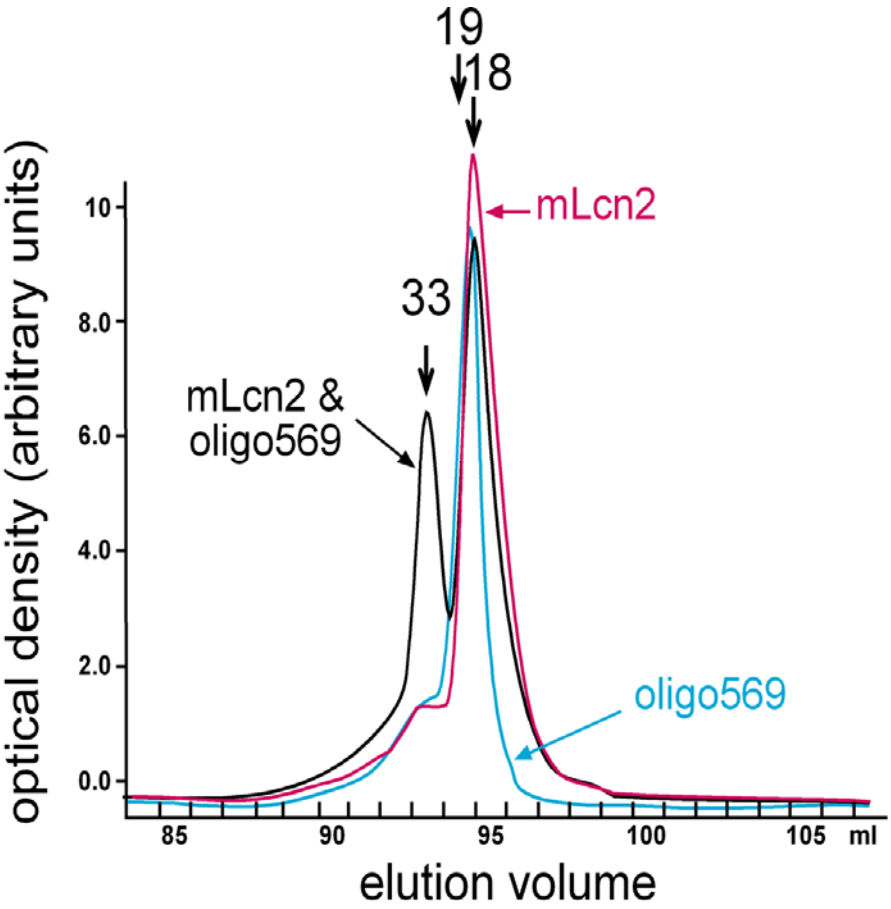
19
18
mLcn2
33
mLcn2 &
oligo569
oligo569
optical density (arbitrary units)
10
8.0
6.0
4.0
2.0
0.0
85
90
95
100
105
ml
elution volume

Figure S4

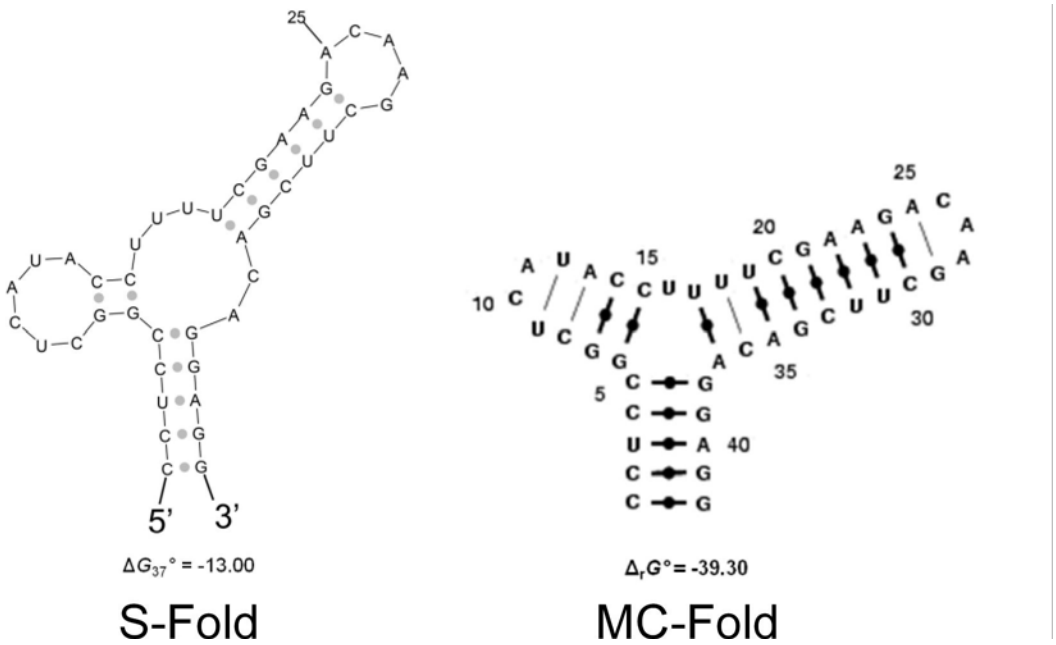

Figure S5

MC-Fold predictions

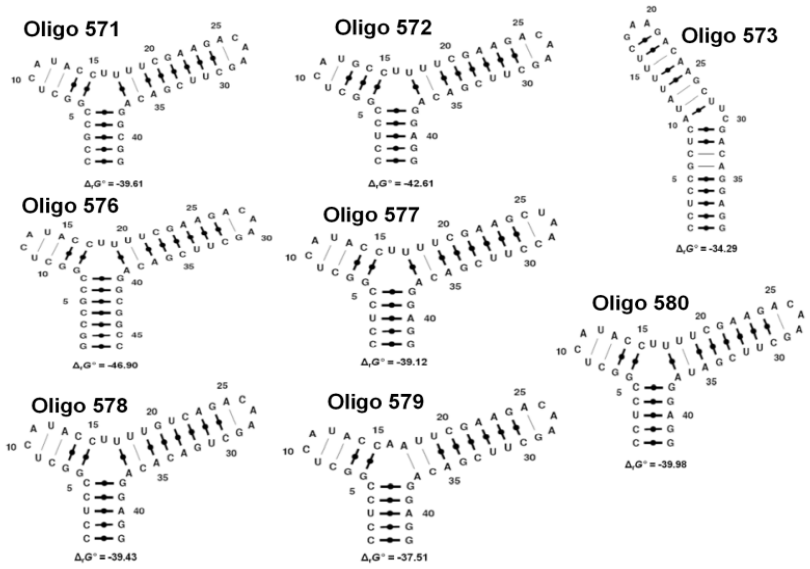

S-Fold predictions

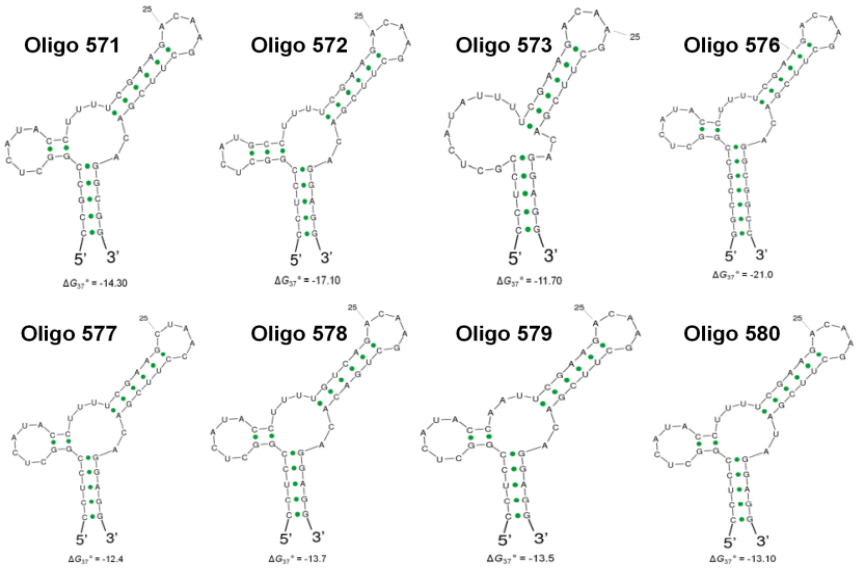

Figure S6

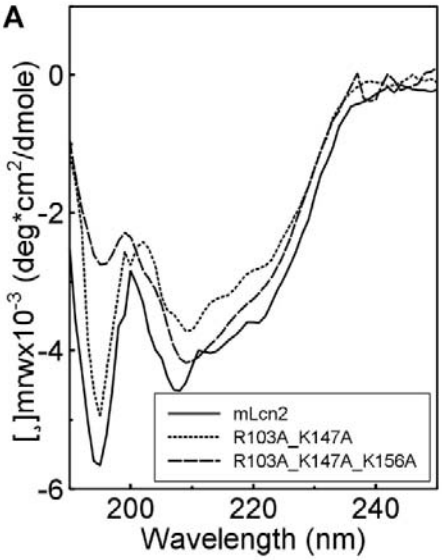

B

protein	Rfac %	helix %	sheet %	coil %
mLcn2	22 ± 5.5	1.4 ± 2.0	47 ± 3.1	51 ± 2.8
R103A_K147A	24 ± 4.6	3.3 ± 2.7	44 ± 5.7	52 ± 4.4
R103A_K147A_K156A	25 ± 2.7	3.4 ± 3.4	45 ± 5.0	52 ± 3.0

Figure S7

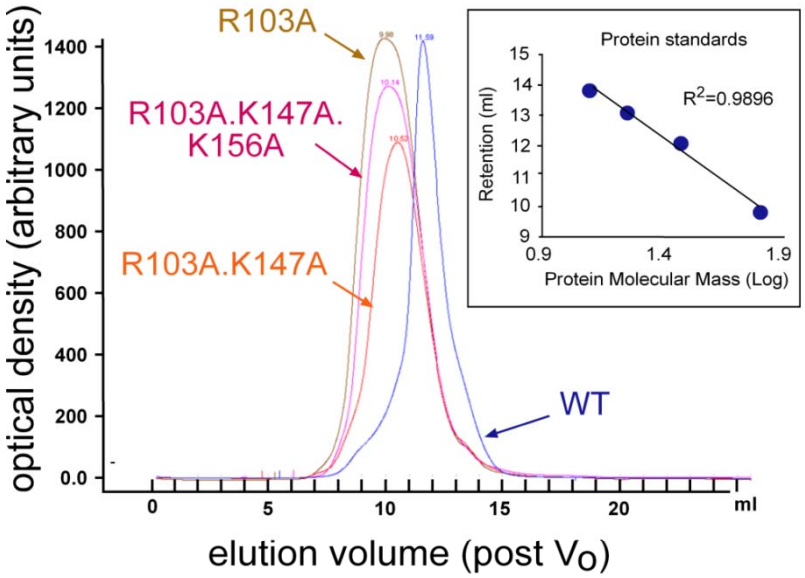
R103A
R103A.K147A.
K156A
R103A.K147A
WT
optical density (arbitrary units)
1400
1200
1000
800
600
400
200
0.0
0
5
10
15
20
ml
elution volume (post Vo)
Protein standards
R2=0.9896
Retention (ml)
15
14
13
12
11
10
9
0.9
1.4
1.9
Protein Molecular Mass (Log)

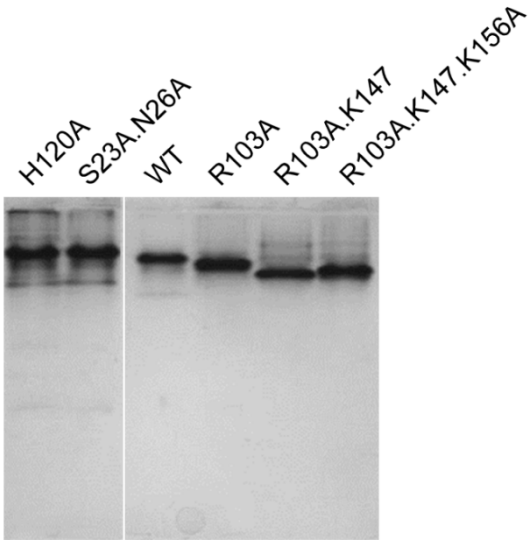
H120A
S23A.N26A
WT
R103A
R103A.K147
R103A.K147.K156A

Figure S8

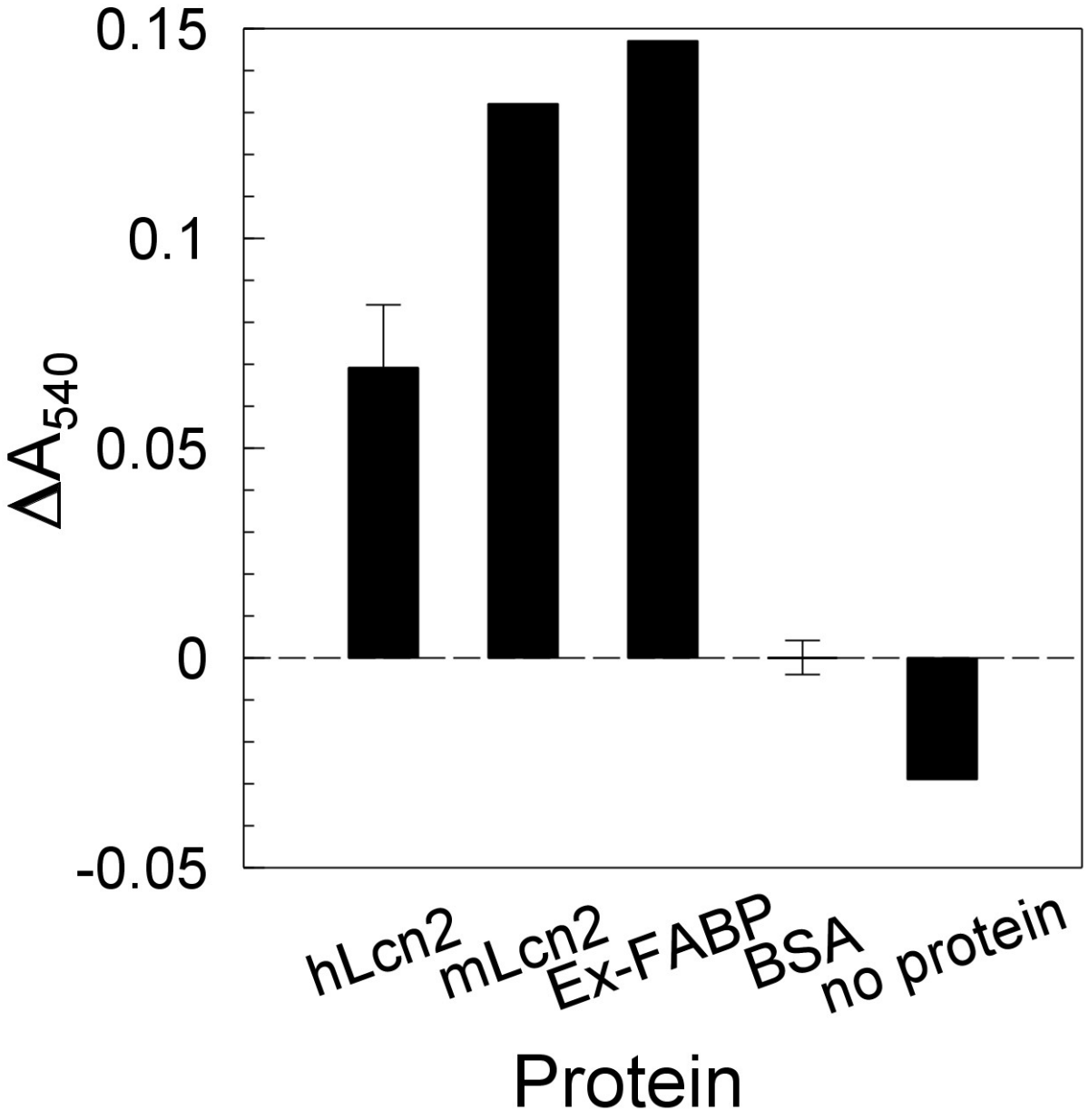
0.15
0.1
0.05
0
-0.05
ΔA540
hLcn2
mLcn2
Ex-FABP
BSA
no protein
Protein

Figure S9

```
        1         10        20        30        40        55
mLcn2   MALSVMCLGLALLGVLQSQAQDSTQNLIPAPSLLTVPLQPDFRSDQFRGRWYVVG
hLcn2   MPLGLLWLGLALLGALHAQAQDSTSDLIPAPPLSKVPLQQNFQDNQFQGKWYVVG

        56                70        80        90        100       110
mLcn2   LAGNAVQKKTEGSFTMYSTIYELQENNSYNVTSILVRDQDQGCRYWIRTFVPSSR
hLcn2   LAGNAILREDKDPQKMYATIYELKEDKSYNVTSVLFRKK--KCDYWIRTFVPGCQ

        111       120       130       140       150       165
mLcn2   AGQFTLGNMHRYPQVQSYNVQVATTDYNQFAMVFFRKTSENKQYFKITLYGRTKE
hLcn2   PGEFTLGNIKSYPGLTSYLVRVVSTNYNQHAMVFFKKVSQNREYFKITLYGRTKE

        166               180       190       200
mLcn2   LSPELKERFTRFAKSLGLKDDNIIFSVPTDQCIDN
hLcn2   LTSELKENFIRFSKSLGLPENHIVFPVPIDQCIDG
```